Fluorescence Studies of a Single Tyrosine in a Type II DNA Binding Protein†

Torleif Härd,‡,§ Victor Hsu,‡ Michael H. Sayre,∥ E. Peter Geiduschek,∥ Krzysztof Appelt,∥,⊥ and David R. Kearns*,‡

Department of Chemistry and Department of Biology and Center for Molecular Genetics, University of California at San Diego, La Jolla, California 92093-0342

Received December 17, 1987; Revised Manuscript Received August 11, 1988

ABSTRACT: We studied the fluorescence properties of a single tyrosine (Tyr94) located in the C-terminal tail of transcription factor 1 (TF1), a type II procaryotic DNA binding protein encoded by the *Bacillus subtilis* phage SPO1. The time-resolved fluorescence intensity of Tyr94 in free TF1 dimers decays as a single exponential, and this is consistent with a twofold symmetrical structure. The fluorescence is readily quenched by acrylamide, but it is less accessible to anionic quenchers (iodide and citrate), suggesting that the tyrosine is located on the protein surface in a negatively charged environment provided by neighboring Glu95 and Asp96 residues. TF1 dimers associate at moderate concentrations (>0.02 mg/mL) as judged from concentration dependencies in the molar fluorescence intensity, the steady-state fluorescence polarization, and the bimolecular quenching constants. Nonspecific binding of TF1 to SPO1 and calf thymus (CT) DNA and to various double-stranded polynucleotides quenches the Tyr94 fluorescence to varying extent. Fluorescence lifetimes of TF1 in the bound state correlate with spectral overlaps between TF1 emission and DNA absorption, demonstrating that excitation energy transfer to DNA bases contributes significantly to the observed quenching. From analysis of the observed quenching in the DNA complexes we conclude that Tyr94 is located within 10–14 Å of the DNA helix axis and not in direct contact with the DNA bases. Equilibrium analyses based on fluorescence titrations show that the maximum binding density on DNA extrapolates to ca. 1 TF1 dimer/5 DNA base pairs. We find several differences in TF1 binding to SPO1 DNA, which contains hydroxymethyluracil instead of thymine, and CT DNA: (i) The tyrosine residue is less exposed to the solvent in the SPO1 DNA complex than in the CT DNA complex. (ii) D_2O addition enhances the Tyr94 fluorescence when TF1 binds to SPO1 DNA but not when it binds to CT DNA. (iii) The TF1–SPO1 DNA complex is stable at higher NaCl concentrations than is the TF1–CT DNA complex, and its formation involves the dissociation of more Na^+ ions than does the TF1–CT DNA complex. On the basis of these observations and the fact that the Tyr94-containing tail of TF1 is essential for binding to SPO1 DNA, we discuss various models for the TF1–DNA complex.

The transcription factor 1 (TF1)[1] protein, encoded by the *Bacillus subtilis* phage SPO1, is a member of the family of type II DNA binding proteins (DBPII; also called HU proteins) (Johnson & Geiduschek, 1972, 1977; Greene et al., 1984; Greene & Geiduschek, 1985a). DBPII from different procaryotes show a high degree of sequence identity. The structure of the DBPII from *Bacillus stearothermophilus* (Dijk et al., 1983) has been solved by X-ray crystallography (Tanaka et al., 1984). It was found to be dimeric with a tightly packed body from which a disordered loop (the "arm") extends, probably in the form of two strands of antiparallel β-sheet (Figure 1A). A structure of the DNA–protein complex in which the two arms of the protein dimer bind in the DNA major groove has been suggested (Tanaka et al., 1984).

TF1 is also a dimer (M_r 23 000) (Johnson & Geiduschek, 1972). It binds to both specific and nonspecific sites in the SPO1 genome, a DNA that contains hydroxymethyluracil (hmUra) in place of thymine (Johnson & Geiduschek, 1977; Greene & Geiduschek, 1985a). This is in contrast to other DBPII proteins, which are thought to exhibit only nonspecific binding [with the exception of *Escherichia coli* integration host factor (IHF)] (Greene et al., 1987). The specific binding might arise from differences in the DNA binding arms of the TF1 dimer or from its unique nine amino acid "tail" (amino acids 91–99) at the protein C-terminus (Greene et al., 1984). (The sequences of TF1 and HU protein are compared in Figure 1B.) Recent studies (Sayre & Geiduschek, 1988) indicate that the nine C-terminal amino acids are essential for binding of TF1 to SPO1 DNA, and these studies raise the possibility that the tail directly interacts with DNA bases in TF1–DNA complexes.

The TF1 tail contains a single tyrosine in position 94, thus making this protein particularly suitable for fluorescence studies. The fluorescence of aromatic amino acids is widely used to probe protein–DNA interactions (Bulsink et al., 1985; Libertini & Small, 1985; Bujalowski & Lohman, 1987; de Jong et al., 1987). Pioneering work in this field was done by Hélène and co-workers, who conducted systematic studies of the binding of small tyrosine- and tryptophan-containing peptides to DNA and proposed that these amino acid residues interact with single- and double-stranded polynucleotides

† This work was supported by grants from NSF (to D.R.K.) and the American Cancer Society (to E.P.G.). T.H. acknowledges a postdoctoral fellowship of the Swedish Natural Sciences Research Council, M.H.S. acknowledges a predoctoral fellowship of the National Science Foundation, and V.H. was a trainee of a NIGMS Cell and Molecular Biology Training Grant.

‡ Department of Chemistry.

§ Present address: Department of Medical Biophysics, Karolinska Institute, Box 60400, S-10401 Stockholm, Sweden.

∥ Department of Biology and Center for Molecular Genetics.

⊥ Present address: Agouron Institute, 505 Coast Blvd., La Jolla, CA 92037.

[1] Abbreviations: TF1, transcription factor 1; DBPII, type II DNA binding protein; CT, calf thymus; bp, base pair; FPA, fluorescence polarization anisotropy; hmUra, hydroxymethyluracil; EDTA, ethylenediaminetetraacetic acid; PMSF, phenylmethanesulfonyl fluoride; Tris, tris(hydroxymethyl)aminomethane; SDS, sodium dodecyl sulfate.

0006-2960/89/0428-0396$01.50/0

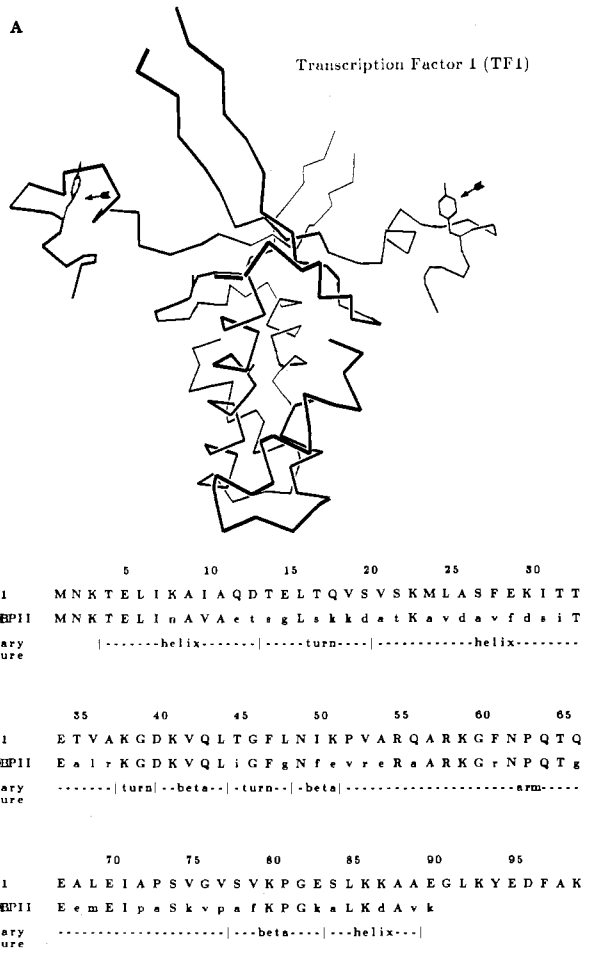

FIGURE 1: (A) Backbone structure of the *B. stearothermophilus* type II DNA binding protein dimer (HU protein) (Tanaka et al., 1984) where the nine amino acids of the TF1 tail (arbitrary conformation) are added to the C-terminus. The Tyr94 residues are indicated with arrows. (B) Amino acid sequences of TF1 and of the *B. stearothermophilus* HU protein (Green et al., 1984). Sequence identities are indicated by capital letters on the second line. Elements of secondary structure in HU are also indicated.

through stacking (single-stranded polynucleotides only) or hydrogen bonding (Hélène, 1971; Hélène & Dimicoli, 1972; Sellini et al., 1973; Brun et al., 1975). Considerable effort has also been made to unambiguously relate various effects (quenching, energy transfer, and D_2O enhancements) to specific interactions of tyrosine and tryptophan with DNA (Feitelson, 1964; Stryer, 1966; Montenay-Garestier, 1975; Alev-Behmoaras et al., 1979).

In the present work we study the fluorescence properties of Tyr94 in TF1 and TF1–DNA complexes to examine the solvent accessibility of the TF1 tails, the aggregation of TF1 dimers, the interaction of TF1 with DNA, and the DNA-induced quenching of the Tyr94 fluorescence. We use these results to obtain structural details of the (nonspecific) TF1–DNA complex. We employ steady-state and time-resolved techniques to monitor changes in the fluorescence intensity of Tyr94 upon intermolecular association and DNA binding. The effects of fluorescence quenchers are then used to compare solvent accessibility in the free and bound states of TF1. We also present equilibrium studies based on fluorescence measurements from which the binding site density for nonspecific binding can be extracted and analyze the effect of Na^+ on the stability of TF1–DNA complexes. On the basis of our observations, we discuss the mechanism of fluorescence quenching in the TF1–DNA complex, various models for TF1 binding to DNA, and possible differences in the interactions with calf thymus (CT) and the hmUra-containing SPO1 DNA.

Materials and Methods

Materials. TF1 was purified from *E. coli* HB101 overexpressing the cloned TF1 gene at 42 °C. The expression plasmid contained a 524 base pair (bp) *Hgi*A1–*Eco*RI fragment containing the TF1 gene (Greene et al., 1984) inserted into the multiple cloning site of the expression vector pKJB842 (Buckley, 1985). In this construct, the TF1 gene is placed downstream of the phage λ rightward promoter and operator. pKJB842 also encodes a thermosensitive λ cI repressor (ts857). Bacteria transformed with this plasmid were grown at 30 °C with aeration in L broth (Miller, 1972) and 100 μg/mL ampicillin to an absorbance of approximately 1 at 600 nm and then shifted to 42 °C and grown for a further 90 min. The cells were collected by centrifugation and quickly frozen at −70 °C. All further manipulations were carried out at 0–4 °C.

Sixty grams of cells was resuspended for washing in 200 mL of buffer A (25 mM Tris-HCl, pH 7.5, 20 mM NaCl, 5 mM $MgCl_2$, 3 mM β-mercaptoethanol, 0.1 mM PMSF), centrifuged, and resuspended in 100 mL of buffer A with 5 μg/mL DNase I for breakage in a French pressure cell at 9000 lb/in^2. The lysate was cleared by centrifugation at 15000*g* for 10 min, and the sediment was discarded. The supernatant was adjusted to 2.1% (w/v) streptomycin sulfate, stirred for 20 min, centrifuged for 15 min at 12000*g* and the sediment was again discarded. The supernatant was diluted with an equal volume of buffer A, and solid $(NH_4)_2SO_4$ was added to 55% saturation [351 mg of $(NH_4)_2SO_4$/mL, stirred for 20 min, and centrifuged for 15 min at 15000*g* with the sediment again discarded. To each milliliter of supernatant, 141 mg of $(NH_4)_2SO_4$ was added (to 75% saturation). The precipitate that formed during 20 min of stirring was collected, dissolved in 50 mL of buffer B (25 mM Tris-HCl, pH 7.5, 70 mM NaCl, 3 mM β-mercaptoethanol, 0.1 mM PMSF), dialyzed against buffer B overnight, and applied to a 30-mL heparin–Sepharose column equilibrated with buffer B. The protein was eluted with a 450-mL linear 0.07–1.4 M NaCl gradient in buffer B. Fractions were analyzed for their protein content by SDS gel electrophoresis. Peak fractions of TF1, eluting at 0.8–1.0 M NaCl, were pooled, dialyzed against buffer C (20 mM Tris-HCl, pH 7.5, 20 mM NaCl, 0.1 mM EDTA), and stored at −70 °C. Protein concentrations were determined by absorbance, using ϵ_{280} = 3000 M(TF1 dimers)$^{-1}$ cm^{-1}. SPO1 DNA was purified from purified phage by extraction with phenol and the concentration determined by using ϵ_{260} = 13 200 M(bp)$^{-1}$ cm^{-1}.

Calf thymus (CT) DNA, purchased from Sigma (type I), was dissolved by mild shearing in the experimental buffer (50 mM NaCl 10 mM Tris-HCl, 2 mM Na_2EDTA at pH 7) and extracted twice with equal volumes of 49% phenol, 49% $CHCl_3$, and 2% isoamyl alcohol (saturated with buffer) and then with ether to remove residual phenol. The DNA was then precipitated in 60% ethanol, centrifuged, dried, and redissolved in buffer to a concentration of 2.7 mM DNA bp as measured by absorbance [using ϵ_{260} = 13 200 M(bp)$^{-1}$ cm^{-1}]. These DNA samples did not show any gross protein contamination, as judged from the absorbance ratio $A_{260}/A_{280} \approx 2.0$, but they did show some residual fluorescence reminiscent of tyrosine emission ($\lambda_{exc} \approx 275$ nm, $\lambda_{em} \approx 305$ nm) with an intensity comparable to the water Raman scattering at a concentration of ≈ 60 μM (bp) DNA. This "background", usually <20% of the total fluorescence intensity, was subtracted in all experiments.

Double-stranded polynucleotides poly(dAdU), poly(dAI^{5}dU), poly(dIdC), and poly(dIBr^{5}dC) were purchased from Pharmacia, Inc., and dissolved in the experimental buffer. Concentrations were determined by using the following extinction coefficients at 260 nm; 11 800, 7500, 7400, and 5000 M(bp)$^{-1}$ cm^{-1} for poly(dAdU), poly(dAI^{5}dU), poly(dIdC), and poly(dIBr^{5}dC), respectively. (These extinction coefficients are based on specifications given by Pharmacia.)

Absorption spectra of the various DNAs (Figure 6A) were measured on a Perkin-Elmer Lambda 4C spectrophotometer and normalized to the extinction coefficients at 260 nm given above.

DNA–protein samples were prepared by adding appropriate amounts of DNA stock solutions to prediluted TF1 solutions. L-Tyrosine, obtained from Sigma, was dissolved in the experimental buffer without further purification. All experiments, except the D_2O studies, were carried out in the same buffer: 50 mM NaCl, 10 mM Tris-HCl, and 2 mM Na_2EDTA at pH 7. The buffers used in the D_2O studies were 50 mM NaCl, 0.5–1.0 mM Tris-HCl, 0.1–0.2 mM Na_2EDTA, and 80–86% D_2O. [The D_2O samples were prepared by diluting the experimental buffer (at pH 7) with D_2O and adding concentrated NaCl to adjust the ionic strength to 50 mM NaCl.] All experiments were performed at room temperature (22–23 °C).

Fluorescence Measurements. Steady-state fluorescence was measured on a SPF-500 Aminco spectrofluorometer. Background emission (<20%) was corrected for by subtracting signals from blank buffer or DNA plus buffer samples. Fluorescence intensities of free TF1 (Figure 4) were also corrected for optical "filtering" effects (<10%) at high TF1 or DNA concentrations. Glan-Thompson prism polarizers were placed in the excitation and emission paths to measure fluorescence polarization anisotropy (FPA). The steady-state FPA, (r), was calculated from

$$\langle r \rangle = \frac{I_{VV} - GI_{VH}}{I_{VV} + 2GI_{VH}} \tag{1}$$

where the subscripts refer to vertical or horizontal positionings of the excitation and emission polarizers, respectively, and $G = I_{HH}/I_{HV}$ is used to correct for polarizing effects in the emission monochromator and the detector. The denominator of eq 1 is proportional to the fluorescence intensity.

The time-correlated single-photon counting instrument used to measure time-resolved fluorescence has recently been described elsewhere (Skibsted et al., 1987). For excitation of tyrosine we use the 514.5-nm line of an actively mode locked Ar^+ laser to pump a rhodamine-110 tunable dye laser generating light at 560 nm, which is frequency-doubled to 280 nm and passed through a cavity dumper to obtain a convenient pulse repetition rate (<10 MHz). The emission was monitored at 310 nm (5-nm bandpass in the monochromator). Emission decay profiles were collected for parallel and perpendicular polarizations of the emitted light (corresponding to I_{VV} and I_{VH}, respectively). Residual DNA fluorescence was measured by using blank DNA samples and subtracted before fitting. The Raman scattering of water (recorded at the same excitation and emission wavelengths, but without an emission polarizer) was used as the instrument response function, $e(t)$, in the deconvolution. The width of the response function at half-maximum was 0.2–0.4 ns.

Deconvolution of Fluorescence Decays. Before deconvolution, a correction factor, G, was calculated from the corrected steady-state anisotropy of the sample and the integrated parallel and perpendicular components of the decay. The truncation errors in the integration were estimated to result in an error in G of <0.1% (assuming a 2-ns fluorescence lifetime). The observed intensity decays were calculated as $I_{obs}(t) = I_{VV}(t) + 2GI_{VH}(t)$. Theoretical expressions for $I(t)$ were then convoluted with the instrument response function and fitted to the observed decays by using

$$I_{obs}(t) = \int_0^t e(t - t')I(t')\,dt' \tag{2}$$

and a nonlinear least-squares fitting program based on the Marquardt algorithm (Press et al., 1986). Estimated standard deviations were taken as derived by Wahl (1979). The fits were judged from reduced χ_r^2 values and from plots of weighted residuals (O'Connor & Phillips, 1984).

Analysis of Excitation Energy Transfer. The rate of excitation energy transfer (Förster, 1984; Lakowicz, 1984), k_{ET}, between an excited donor (e.g., Tyr94 in TF1) and an acceptor in the ground state (a DNA base) is given by

$$k_{ET} = \frac{\kappa^2 \phi_D J}{r^6 n^4 \tau_D}(8.71 \times 10^{23})\ s^{-1} \tag{3}$$

where ϕ_D is the quantum yield of the donor in the absence of the acceptor, n is the refractive index of the medium, r is the distance between donor and acceptor (in Å), κ^2 is an orientation factor reflecting the relative orientation of the donor and acceptor transition moments, τ_D is the measured fluorescence lifetime of the donor in the absence of the acceptor, and J is the spectral overlap between donor emission and acceptor absorption (in M^{-1} cm^3). The spectral overlap is defined as

$$J = \frac{\int_0^\infty F_D(\lambda)\epsilon_A(\lambda)\lambda^4\,d\lambda}{\int_0^\infty F_D(\lambda)\,d\lambda} \tag{4}$$

where $\epsilon_A(\lambda)$ is the extinction coefficient of the acceptor (DNA) and $F_D(\lambda)$ is the relative fluorescence intensity of the donor (Tyr94 in TF1) at the corresponding wavelength λ. A critical distance, R_0, for energy transfer, at which $k_{ET} = 1/\tau_D$, is usually calculated from eq 3.

If $(\kappa^2\phi_D)/(r^6n^4)$ is constant in TF1 complexes with different DNAs (with different absorption spectra), then a plot of the observed relative fluorescence quantum yields of free and bound TF1, ϕ_f/ϕ_b, versus the spectral overlap, J (Figure 6B), is expected to result in a linear dependence described by

$$\frac{\phi_f}{\phi_b} = \frac{\dfrac{\Gamma}{\Gamma + k_f}}{\dfrac{\Gamma}{\Gamma + k_b + k_{ET}}} = \frac{\Gamma + k_b}{\Gamma + k_f} + \tau_f k_{ET} = \frac{\Gamma + k_b}{\Gamma + k_f} + \frac{\kappa^2 \phi_f}{r^6 n^4}(8.71 \times 10^{23})\,J \tag{5}$$

where $1/\Gamma$ is the natural fluorescence lifetime, τ_f is the observed fluorescence lifetime of free TF1, k_f and k_b are nonradiative decay rates (other than energy transfer), and ϕ_f and ϕ_b are (observed) fluorescence quantum yields in free and bound TF1, respectively.

Analysis of Quenching Experiments. The classical Stern–Volmer equations for collisional quenching describes the decrease in fluorescence intensity as a function of quencher concentration, [Q]

$$\frac{F_0}{F} = 1 + k_q\tau_0[Q] \tag{6}$$

where F_0 is the initial fluorescence intensity, F is the intensity in the presence of added quencher (corrected for quencher

absorption), τ_0 is the fluorescence lifetime in the absence of quencher, and k_q is the bimolecular rate constant for quenching. The observed fluorescence decrease in a sample containing two fluorescent species (bound and free protein) with different lifetimes and quenching constants can be written as (Eftink & Ghiron, 1976)

$$\frac{F_0}{F} = \frac{(R + 1)(1 + k_{q,f}\tau_{0,f}[Q])(1 + k_{q,b}\tau_{0,b}[Q])}{1 + k_{q,f}\tau_{0,f}[Q] + R(1 + k_{q,b}\tau_{0,b}[Q])} \quad (7)$$

where the subscripts denote free and bound species, $R = \alpha_f\tau_{0,f}/\alpha_b\tau_{0,b}$ is the ratio between the fluorescence intensities of the two species in the absence of quencher, and the α's represent the fractions of free and bound protein, respectively. Equation 4 was fitted to experimental data for DNA–protein samples by using a nonlinear least-squares routine with R and $k_{q,b}$ as variables or with $k_{q,b}$ as the only variable and R derived from binding isotherms. The parameters $\tau_{0,f}$, $\tau_{0,b}$, and $k_{q,f}$ were all obtained from appropriate experiments.

Equilibrium Studies. Binding isotherms for the TF1–DNA equilibrium were obtained from titrations of DNA with protein, keeping the DNA concentration constant, and from titrations of protein with DNA at constant protein concentration ("reverse" titrations). The fluorescence intensity was corrected for protein and DNA absorption, and the fractional quenching was calculated as $Q = (I_0 - I)/I_0$, where I_0 is the fluorescence intensity of free protein and I is the observed intensity of the DNA–protein sample (at the same total protein concentration). The reverse titrations give an indication of the relative strength of nonspecific complexes between TF1 and different DNAs, and they also provide an estimate of the maximum quenching, $Q_{max} = (i_{free} - i_{bound})/i_{free}$, where i_{free} and i_{bound} are molar fluorescence intensities in the free and bound state, respectively. This estimate is compared to the measured fluorescence lifetimes of the free and bound states and used to calculate the extent of bound protein at various protein concentrations, using $C_{bound} = Q/Q_{max}C_{tot}$. Fluorescence titrations of this type can, in principle, be used to construct Scatchard plots (Cantor & Schimmel, 1980) to determine binding site densities, equilibrium constants, and cooperativity parameters. However, such an analysis would be uncertain in our case because the aggregation equilibrium (see Results) between free protein ligands is not known in detail, and this information is needed if the true free ligand concentration is to be determined. Note also that our method of calculating the concentration of bound protein is not justified if different binding modes result in different fluorescence quantum yields. Bujalowski and Lohman recently published an ingenious method to deal with this problem (Bujalowski & Lohman, 1987). Unfortunately, their method is not applicable when the protein forms aggregates. In view of these potential problems we only use data obtained at high binding ratios to estimate the binding site density (n) for TF1 dimers on DNA, assuming that a single mode of protein binding dominates at high binding ratios. This was done by plotting $1/C_{bound}$ versus $1/C_{tot}$ for data from titrations at constant DNA concentrations, and obtaining the binding site density from the value of $1/C_{bound}$ extrapolated to $1/C_{tot} = 0$. This method can be expected to yield an accurate estimate of the binding site density as long as the free ligand concentration increases with the total protein concentration, i.e., when the equilibrium constant for protein–protein association is finite.

Analysis of Salt Effects on Binding. TF1–DNA samples were titrated with concentrated NaCl solutions keeping TF1, DNA, and buffer concentrations constant. The free and bound protein concentrations were determined as described above,

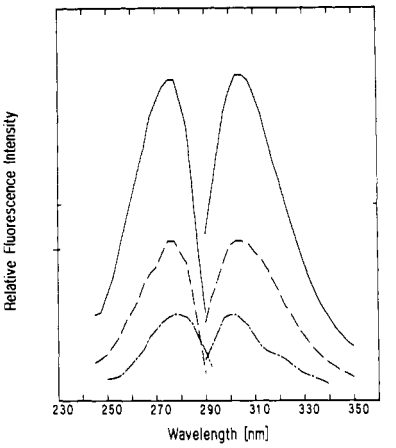

FIGURE 2: Fluorescence excitation (λ_{em} = 302 nm) and emission (λ_{exc} = 275 nm) spectra of free and bound TF1: (—) Free TF1 (1.7 μM dimers); (---) TF1 bound to CT DNA [3.0 μM TF1 dimers, 63 μM (bp) DNA]; (-·-) TF1 bound to SPO1 DNA [2.5 μM TF1 dimers, 57 μM (bp) DNA]. The spectra are normalized to the molar fluorescence intensity of free TF1.

and an "observed" binding constant (neglecting overlap between binding sites), K_{obs}, was calculated from

$$K_{obs} = \frac{[TF1_b]}{[TF1_f](C_{DNA}/n - [TF1_b])} \quad (8)$$

where C_{DNA} is the total DNA base pair concentration and n is the binding site density obtained from the equilibrium titrations. The slope of a plot of log K_{obs} versus log [Na^+] is proportional to the number of ions released (in a thermodynamic sense) when the complex is formed. Assuming that Manning's ion condensation hypothesis is valid, Record et al. (1976a; deHaseth et al., 1977) showed that K_{obs} is related to the cation (Na^+) concentration as

$$-\frac{\partial \log K_{obs}}{\partial \log [Na^+]} = m'\psi \quad (9)$$

where m' is the number of Na^+ ions released upon protein binding and ψ is a thermodynamic Na^+ binding parameter calculated to be $\psi = 0.88$ for double-helical DNA (Record et al., 1976a,b). Salt titrations of this kind are frequently used to estimate the number of ionic contacts in DNA–protein complexes (deHaseth et al., 1977; Kowalczykowski et al., 1981; Khrapunov et al., 1984; Bulsink et al., 1985; de Jong et al., 1987), although it should be noted that our neglect of binding site overlap in eq 8 will affect K_{obs} differently depending on the binding density. Because of this effect we performed salt titrations at different initial binding densities, and we also focus our attention on differences between CT and SPO1 DNA, rather than on absolute numbers obtained in the analysis.

Results

Free Protein. Fluorescence excitation and emission spectra of Tyr94 in TF1 are shown in Figure 2. The excitation and emission maxima, positioned at approximately 278 and 305 nm, respectively, are slightly red-shifted compared to those of L-tyrosine (275 and 302 nm, data not shown), but there is no indication of broadening of the emission peak—the width at half-maximum is about 35 nm as with L-tyrosine. These spectral properties indicate that the Tyr94 residue is not involved in hydrogen-bonded complexes with nearby proton acceptors (other than water molecules), because such complexes would be expected to result in a broadening of the emission spectrum due to fluorescence from a "tyrosinate-like" species (Lakowicz, 1984). Figure 3A shows the time-resolved

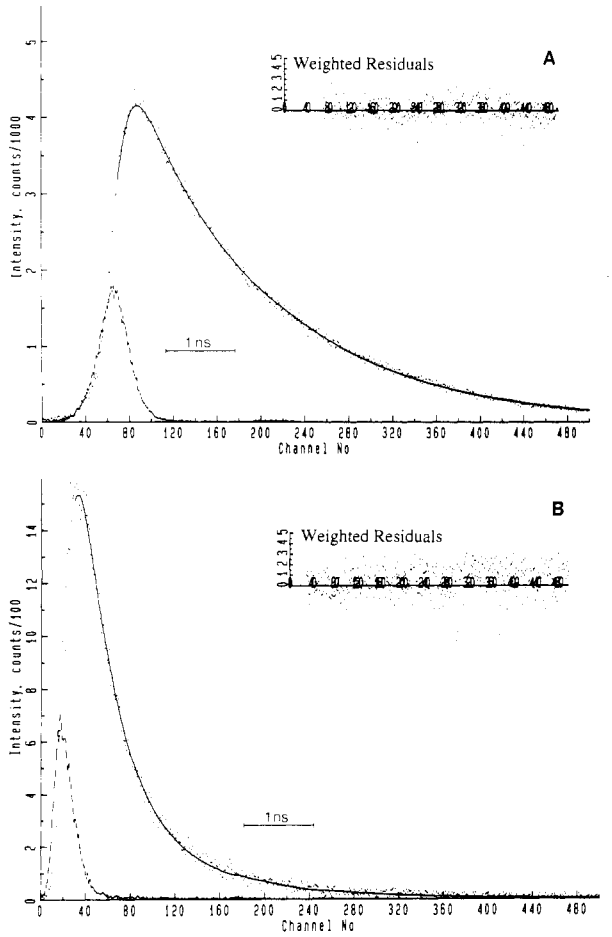

FIGURE 3: Time-resolved fluorescence of free and bound TF1. (A) TF1 (9.0 μM TF1 dimers); (B) TF1 bound to SPO1 DNA [9.0 μM TF1 dimers and 57 μM (bp) SP01 DNA]. The instrument response function and best-fit deconvolutions with single- (free TF1) and double-(TF1/SPO1 DNA) exponential decays (with weighted residuals) are indicated. Best-fit decay parameters are shown in Table I.

Table I: Fluorescence Intensity Decay Parameters for Free and Bound TF1[a]

sample	lifetimes[b] (ns)	amplitudes[b] (%)	χ_r^2	Q_{max}[b,c]
free TF1	1.93 ± 0.1	100	1.5	
	1.95 ± 0.6	96 ± 2	1.5	
	0.65 ± 1.0	4 ± 2		
TF1/SPO1 DNA	0.50 ± 0.1	90 ± 5	2.3	0.74 ± 0.04
	1.42 ± 0.5	10 ± 3		
	0.38 ± 0.5	59 ± 20	2.3	
	0.79 ± 1.0	39 ± 20		
	2.4 ± 2.0	2 ± 2		
TF1/CT DNA	0.48 ± 0.1	80 ± 5	1.6	0.75 ± 0.04
	1.69 ± 0.5	20 ± 5		
	0.31 ± 0.6	37 ± 10	1.6	
	0.54 ± 1.5	51 ± 5		
	1.77 ± 2.0	12 ± 5		
TF1/poly(dIdC)	0.55 ± 0.05	68 ± 2	1.4	0.72 ± 0.02
	2.00 ± 0.22	32 ± 2		
TF1/poly(dIBr^{5}dC)	0.22 ± 0.05	67 ± 2	1.4	0.88 ± 0.02
	1.81 ± 0.12	33 ± 2		
TF1/poly(dAdU)	0.93 ± 0.05	71 ± 2	1.6	0.52 ± 0.02
	2.1 ± 0.4	29 ± 2		
TF1/poly(dAI^{5}dU)	0.19 ± 0.02	90 ± 4	1.9	0.91 ± 0.01
	3.7 ± 2.7	10 ± 4		

[a] Concentrations are 4–11 μM TF1 dimers and 57–88 μM (bp) DNA. [b] All uncertainties represent estimated standard deviations. [c] Calculated from fits to double-exponential decays using $Q_{max} = 1 - \tau_b/\tau_f$, where $\tau_f = 1.93$ ns.

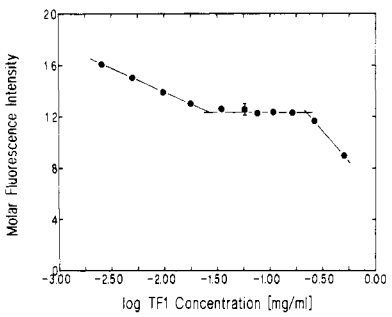

FIGURE 4: Effect of concentration on the molar fluorescence intensity of free TF1. The data are corrected for filtering due to TF1 absorbance. The dashed lines indicate three significant concentration intervals that are discussed in the text.

intensity decay of TF1. The deconvolution yields an acceptable fit to a single-exponential decay with a fluorescence lifetime of 1.9 ns. [The fit is not improved when a double-exponential decay is assumed (Table I).] On the basis of this lifetime and the fluorescence lifetime and quantum yield of tyrosine [$\tau_F = 3.8$ ns (Laws et al., 1986) and $\phi = 0.14$ (Chen, 1967)], we estimate the fluorescence quantum yield of Tyr94 in TF1 to be $\approx$0.07 (at 0.2 mg of TF1/mL).

The molar intensity of TF1 fluorescence is concentration dependent, decreasing with concentration, as shown in Figure 4. The decrease is more pronounced in the concentration interval 2.5–20 μg/mL (20 μg/mL $\approx$ 1 μM dimers) and at concentrations >0.2 mg/mL, whereas the intensity is approximately constant between 0.02 and 0.2 mg/mL. (Most time-resolved fluorescence and TF1–DNA equilibrium data reported here were measured at free TF1 concentrations within this interval.) The decrease in molar fluorescence intensity is attributed to intermolecular association of TF1 dimers. Data obtained at low TF1 concentrations could be complicated by adhesion of TF1 to surfaces (Johnson & Geiduschek, 1974). Loss of material due to this effect would deplete the solution of protein and therefore lead to an underestimate of the molar intensity. Because we observe the opposite behavior (an increase), we conclude that surface adhesion is not the cause of the concentration dependence below 0.02 mg/mL.

The steady-state fluorescence polarization anisotropy (FPA) also varies with the TF1 concentration (data not shown). Over the range from 0.03 mg/mL the FPA increases from ~0.11 to 0.16. While changes in fluorescence lifetime affect the steady-state FPA values, in the "intermediate" concentration range (0.02–0.2 mg/mL), they can still be compared because the average lifetime is approximately constant in this concentration interval. The FPA at 0.13 mg/mL ($\langle r \rangle = 0.13$) is slightly larger than at 0.04 mg/mL ($\langle r \rangle = 0.11$), indicating less rotational mobility (aggregation) at the higher concentration.

Quenching experiments were performed to probe the environment and exposure of the Tyr94 residue to the solvent. Figure 5A shows the effect of acrylamide, NaI, and sodium citrate on the fluorescence intensity of TF1. The rate constants for acrylamide quenching of the TF1 fluorescence (shown in Table II) are high (on the order of 10^{10} M^{-1} s^{-1} for TF1) and comparable to the value obtained for L-tyrosine ($k_q = 0.7 \times 10^{10}$ M^{-1} s^{-1}). This indicates that the quenching of Tyr94 is diffusion-controlled (Lakowicz, 1984) and suggests that this residue is exposed to the solvent on the protein surface. We also find that the quenching of TF1 fluorescence is slightly reduced at higher concentrations (see Table II), suggesting that the tyrosine is less exposed in the aggregated state. The I^- and citrate quenching of L-tyrosine fluorescence is somewhat less efficient than acrylamide quenching (see Table II). The difference might arise from a lower diffusivity of these (hy-

Table II: Effect of Quenchers on Tyrosine Fluorescence

quencher	[TF1] (mg/mL)	$K = k_q\tau_0$ (M^{-1})	τ_0[b](ns)	$10^{-10}k_q$ (M^{-1} s^{-1})
(A) L-Tyrosine[a]				
acrylamide		21.2		0.68
NaI		9.4		0.30
sodium citrate		5.2		0.17
(B) Free TF1				
acrylamide	0.01	26.6	2.2	1.21
	0.033	21.0	2.0	1.05
	0.2	15.3	1.9	0.81
NaI	0.033	2.0	2.0	0.10
sodium citrate	0.033	1.16	2.0	0.06
NaCl	0.033	(no quenching)		

quencher	sample	$R = \alpha_f\tau_{0,f}/\alpha_b\tau_{0,b}$	$10^{-10}k_{q,b}$ (M^{-1} s^{-1})
(C) Bound TF1[c]			
acrylamide	CT DNA	0.79 (fixed)	1.9
		0.8 (varied)	2.0
	SPO1 DNA	0.32 (fixed)	(0.005)[d]
		1.0 (varied)	0.16

[a] Fluorescence lifetime, τ_0 = 3.8 ns. [b] The fluorescence lifetime of the 0.2 mg/mL sample was obtained in a time-resolved measurement. The other lifetimes are calculated by using this value and the molar fluorescence intensities shown in Figure 4. [c] Fits to eq 7 using fluorescence lifetimes as in Table I and $k_{q,f} = 1.2 \times 10^{10}$ M^{-1} s^{-1}. [d] No good fit obtained.

drated) ions in water solution or from a lower "quenching efficiency" in the collision between quencher and fluorophore. The quenching of Tyr94 in TF1 by I^- and citrate is reduced by a factor of ≈3 compared to L-tyrosine. The slower diffusion of TF1 might reduce the quenching by a factor of 2 (at the most), because the bimolecular quenching constant is expected to be proportional to the sum of the diffusivities of the fluorophore and the quencher (Lakowicz, 1984). However, since we observe no major difference in the acrylamide quenching of Tyr94 and L-tyrosine fluorescence, it is more probable that the local environment of Tyr94 in TF1 protects the fluorophore from quenching by anions, possibly owing to a net negative charge provided by neighboring Glu95 and Asp96 residues. The observation that NaCl addition does not affect the Tyr94 emission (Table II) means that we do not have to consider any NaCl dependence in the molar fluorescence intensity of free TF1 when we evaluate the effect of salt on the TF1–DNA equilibrium (Figure 8).

We find that the TF1 fluorescence is enhanced by ≈40% in 80% D_2O (not shown). With tyrosine residues, an isotope effect on the fluorescence indicates base-catalyzed exchange of the tyrosine hydroxyl proton (Stryer, 1966), as discussed below.

TF1–DNA Complexes. The Tyr94 fluorescence is quenched when TF1 binds to calf thymus (CT) or SPO1 DNA (Figure 2). However, other spectral properties of the tyrosine emission (emission maximum and bandwidth) do not change, indicating that the Tyr94 is still hydrogen-bonded to water in the complexes (Lakowicz, 1984). The time-resolved intensity decays of the TF1–DNA samples are double exponential due to the presence of bound and free protein species; the lifetimes are about 0.5 ns in the bound state compared to about 1.9 ns for the free protein (Figure 3B, Table I). The extent of quenching in the TF1–SPO1 sample, $Q = (I_0 - I)/I_0$, calculated from lifetimes and amplitudes in Table I is Q = 0.67, in good agreement with the value of Q = 0.64 obtained from steady-state fluorescence measurements on the same samples of free and bound TF1 (corrected for DNA absorption). Note that as these experiments are carried out at high TF1–DNA ratios

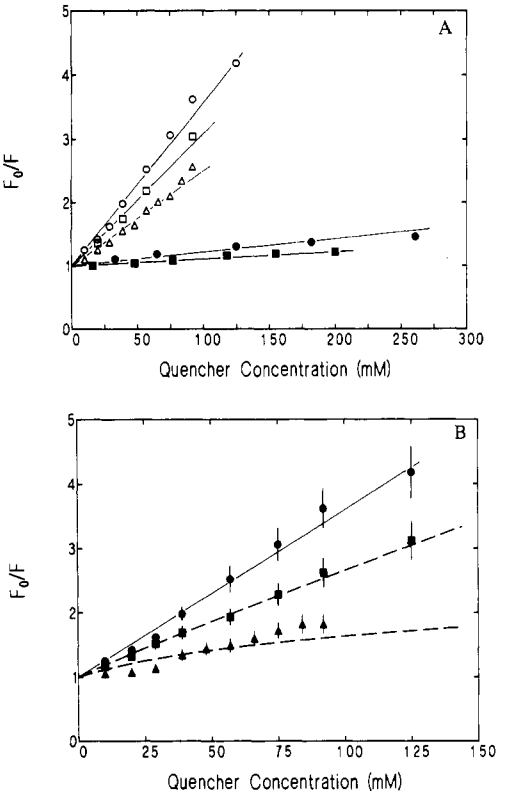

FIGURE 5: Stern–Volmer plots of the quenching of free and bound TF1. (A) Quenching of free TF1 fluorescence by acrylamide [(○) 0.01 mg/mL TF1, (□) 0.033 mg/mL, and (△) 0.2 mg/mL], NaI [(●) 0.033 mg/mL], and sodium citrate [(■) 0.033 mg/mL]. Calculated bimolecular quenching constants are shown in Table II. (B) Quenching of free and bound TF1 fluorescence by acrylamide. The concentrations are (●) 0.43 μM TF1 dimers, (■) 1.0 μM TF1 dimers, 30 μM (bp) CT DNA, and (▲) 1.0 μM TF1 dimers, 28 μM SPO1 (bp) DNA. The lines indicate the best fits of eq 7 to the experimental data with $k_{q,b}$ and R as variables in the fits (fitted values are shown in Table II).

(1 TF1 dimer/15 DNA bp) most proteins are bound to nonspecific sites on the SPO1 DNA (Johnson & Geiduschek, 1977).

There is a difference in the effect of D_2O on the fluorescence of TF1 complexed with SPO1 and CT DNA. With SPO1 DNA, 80% D_2O enhances the fluorescence by ≈40%, as in the free protein. In contrast, there is no D_2O effect when TF1 binds to CT DNA, suggesting that proton exchange is not being catalyzed in the CT DNA–protein complex. This observation, too, is an indication of different binding modes in the two complexes. The absence of catalyzed proton exchange in the TF1–CT DNA complex is not inconsistent with a higher solvent accessibility to Tyr94, because proton exchange with water is too slow to give rise to an isotope effect (Feitelson, 1964), as explained under Discussion.

Calculations of critical distances for excitation energy transfer between tyrosine and the DNA bases show that this mechanism is likely to contribute to quenching of tyrosine fluorescence in DNA complexes (Montenay-Garestier, 1975). To estimate the extent of energy transfer, we studied the time-resolved and steady-state fluorescence of TF1 complexed with double-stranded poly(dIdC) and poly(dAdU), which have absorption properties different from those of SPO1 and CT DNA. The heavy-atom-containing derivatives poly(dAI^5dU) and poly(dIBr^5dC) were also included, because the heavy atoms induce significant red shifts in the absorption spectra and also because a heavy atom effect on the Tyr94 fluorescence (complete quenching) would be expected if the Tyr94 residue were located in direct contact with the DNA major groove.

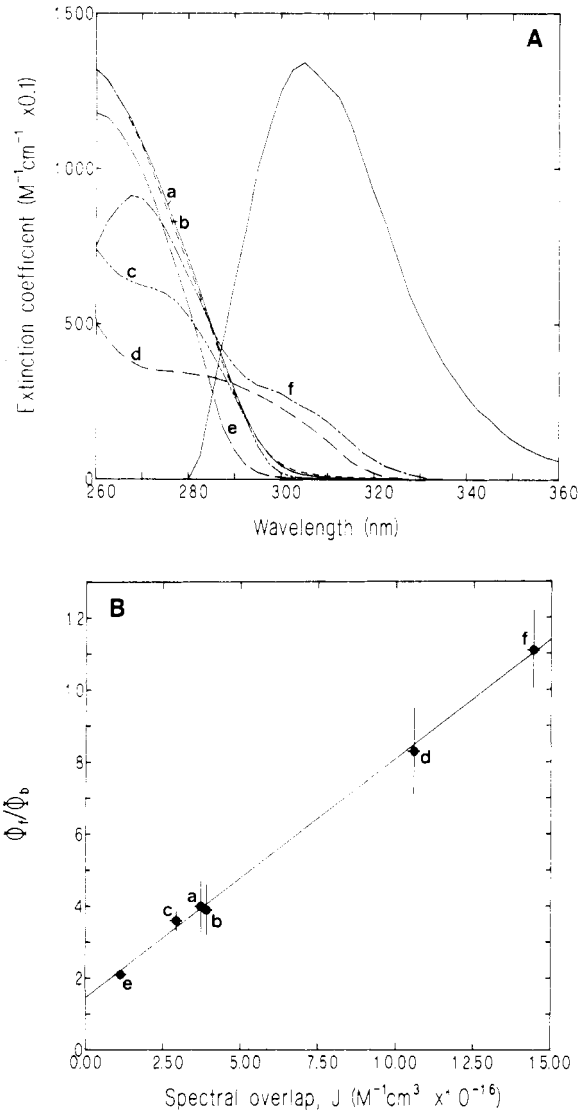

FIGURE 6: (A) Absorption spectra of (a) CT DNA (solid line), (b) SPO1 DNA (dashed line), (c) poly(dIdC), (d) poly(dIBr^{5}dC), (e) poly(dAdU), and (f) poly(dAI^{5}dU) and emission spectrum of TF1 illustrating spectral overlaps between TF1 emission and DNA absorption. (B) Plot of the relative fluorescence quantum yields of free and bound TF1, ϕ_f/ϕ_b, versus the spectral overlap, J, calculated from eq 3. Data points for various DNAs are labeled as in (A). Error bars indicate estimated standard deviations. The solid line represents a least-squares fit of the data to eq 5.

The data in Table I indicate that the fluorescence lifetime of Tyr94 in the bound state is dependent on the DNA sequence, ranging from 0.2 ns with poly(dAI^{5}dU) and poly(dIBr^{5}dC) to 0.9 ns with poly(dAdU). Reverse titrations with TF1 at constant DNA concentrations (not shown) also yield values of Q_{max} that depend on DNA sequence in good agreement with the time-resolved fluorescence data. Figure 6 shows the spectral overlaps between TF1 emission and absorption spectra of the various DNAs and a plot of the observed reduction in relative quantum yields (ϕ_f/ϕ_b) versus spectral overlap integrals calculated from eq 4. The data in Figure 6B fall on a straight line with a substantial slope (0.66×10^{16} cm^{-6}), demonstrating that excitation energy transfer contributes to the quenching of Tyr94 fluorescence in the bound state. A linear least-squares fit of the data in Figure 6B yields an intercept with the abscissa at $\phi_f/\phi_b = 1.4 \pm 0.3$. An intercept of $\phi_f/\phi_b = 1$ would be expected if energy transfer were the only "extra" mechanism of excited-state deactivation in the bound state (all other deactivation rates being the same as in free TF1, i.e., $k_f = k_b$ in eq 5), and it is therefore likely that other processes also contribute to the quenching.

Figure 6B also provides evidence that Tyr94 is not in direct contact with the DNA bases since energy transfer would have completely quenched the emission in every case [even in poly(dAdU) the R_0 = 10 Å] (Montenay-Garestier, 1975). Moreover, the experimental points for the heavy-atom-containing DNAs fall on the same line as do points for non-heavy-atom DNAs, and this indicates that the Tyr94 fluorescence is not totally quenched, as would be expected if it were in direct contact with the heavy atoms in the DNA major groove.

The solvent accessibility of the Tyr94 residue in bound TF1 was studied by means of acrylamide quenching. We find that acrylamide is less effective in quenching the Tyr94 fluorescence in the DNA complexes than in the free protein (Figure 5B), and the data show differences between the complexes with CT and SPO1 DNA. Since these effects might be due to the shorter fluorescence lifetime in the bound state, it is necessary to take into account changes in fluorescence lifetimes upon binding and the fraction of bound protein to calculate bimolecular quenching constants for the TF1–DNA complexes. The data are therefore fitted to eq 7 by using the value of $k_{q,f}$ for the free protein at 0.01 mg/mL and the fluorescence lifetimes in Table I. The fit is carried out in two ways: either by keeping R fixed and using α values from the binding studies (to be described below) and fitting $k_{q,b}$ only or by fitting both R and $k_{q,b}$. With CT DNA good fits are obtained in both cases (Figure 5B and Table II). The bimolecular quenching constants in the free and bound states are comparable (1.2×10^{10} and 1.9×10^{10} M^{-1} s^{-1}, respectively), indicating that the Tyr94 residue is still exposed to the solvent when TF1 binds to CT DNA. With SPO1 DNA it is not possible to fit the data by using an R value obtained from the binding experiments. A better fit is obtained by treating R as a variable, yielding $k_{q,b} = 1.6 \times 10^9$ M^{-1} s^{-1}, which is about 7 times lower than in the free protein. Going back and comparing the fractions of free and bound protein obtained from the fitted R value (α_f and α_b) with the titration in Figure 7B, we find that these are reasonable considering the experimental errors in the binding experiments. On this basis we accept the fit and conclude that Tyr94 is considerably more protected from solvent exposure in the SPO1 complex than in the CT DNA complex. The effects of NaI and sodium citrate as quenchers in the bound state were not investigated because the complexes dissociate when salt is added (Figure 8).

Studies of the TF1–DNA equilibrium based on fluorescence data were carried out to determine the binding site density on DNA and to compare the binding of TF1 to SPO1 and CT DNA. Figure 7A shows the results of a reverse titration with DNA at constant TF1 concentration. It is evident from this figure that the binding to the two different DNAs is quite comparable when nonspecific complexes are formed at low salt concentrations. Values of the observed quenching, Q, obtained at high DNA concentrations provide an estimate of the fluorescence quantum yield of Tyr94 in the bound state. With CT DNA, Q seems to level off at $Q_{max} = 0.75 \pm 0.05$. This value of Q_{max}, which is in good agreement with the fluorescence lifetimes presented in Table I, will be used to estimate the binding site density and when effects of ionic strength on the equilibrium are examined.

Figure 7B shows data from titrations with TF1 at constant DNA concentration, presented as plots of $1/C_{bound}$ versus $1/C_{tot}$, where C_{bound} is calculated from Q and Q_{max} as described under Materials and Methods. The optical concentration of

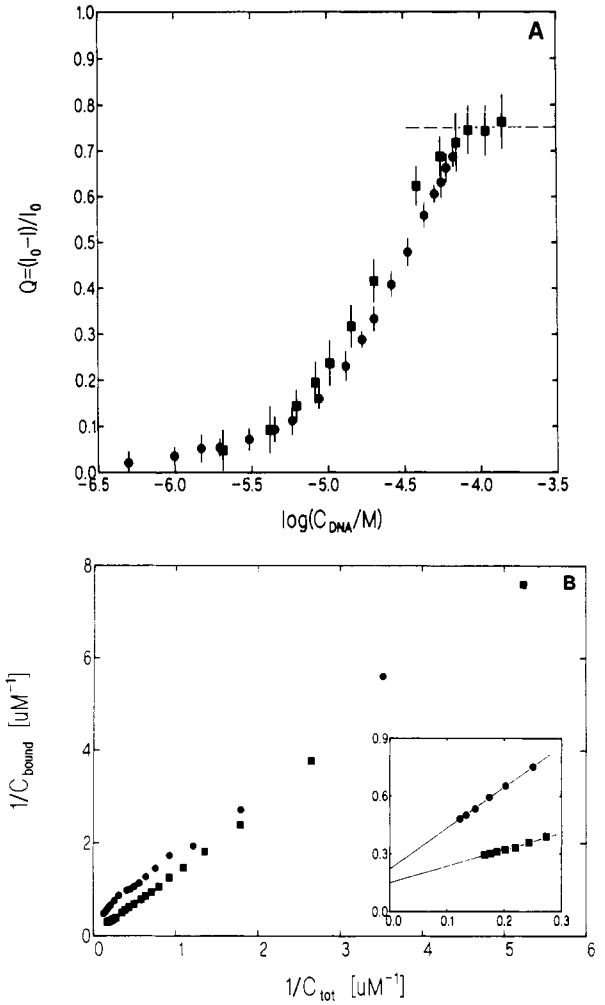

FIGURE 7: Fluorescence titration studies of the TF1–DNA equilibrium. Filled circles and squares represent data obtained with SPO1 and CT DNA, respectively. (A) Reverse titrations of DNA at constant TF1 concentration (4 μM dimers), presented as plots of the observed quenching, $Q = (I_0 - I)/I_0$, versus log C_{DNA}. The dashed line indicates $Q_{max} = 0.75$. (B) Plot of $1/C_{bound}$ versus $1/C_{tot}$ [μM(TF1 dimers)$^{-1}$] obtained from titrations of TF1 at constant DNA concentration [22 μM (bp) SPO1 DNA or 30 μM (bp) CT DNA]. C_{bound} was calculated as described under Materials and Methods by using $Q_{max} = 0.75$. The inserts show data obtained at high TF1 concentrations, where the solid lines represent linear extrapolations used to estimate the binding site density on DNA, as described in the text.

bound TF1 (at the given DNA concentration) can be estimated by extrapolating data points at high binding densities (the insert in Figure 7B) to $1/C_{tot} = 0$. The binding site density can then be calculated as $n = C_{DNA}/C_{bound,max}$ (DNA bp/TF1 dimer). For both SPO1 and CT DNA we obtain $n = 5 \pm 0.5$, where the uncertainty is due to the uncertainty in Q_{max} mentioned above, suggesting that this value is the "packing" limit for TF1 dimers on DNA. It should be noted that other DNA binding proteins exhibit similarly large values: 5 repressor molecules/28 DNA bp for the nonspecific complex between DNA and the *lac* repressor (Lawson & York, 1987) and ≈4–6 nucleotides/molecule of protein for the IKe and M13 gene 5 and the RecA single-stranded DNA binding proteins (Cazenave et al., 1984; de Jong et al., 1987).

The TF1–DNA complexes dissociate at moderate salt concentrations as judged from the increase in the fluorescence intensity upon addition of NaCl (Figure 8). The midpoint of the transition is higher with SPO1 DNA (≈350 mM NaCl) than with CT DNA (≈225 mM) at comparable DNA and protein concentrations, indicating that the SPO1–TF1 complex

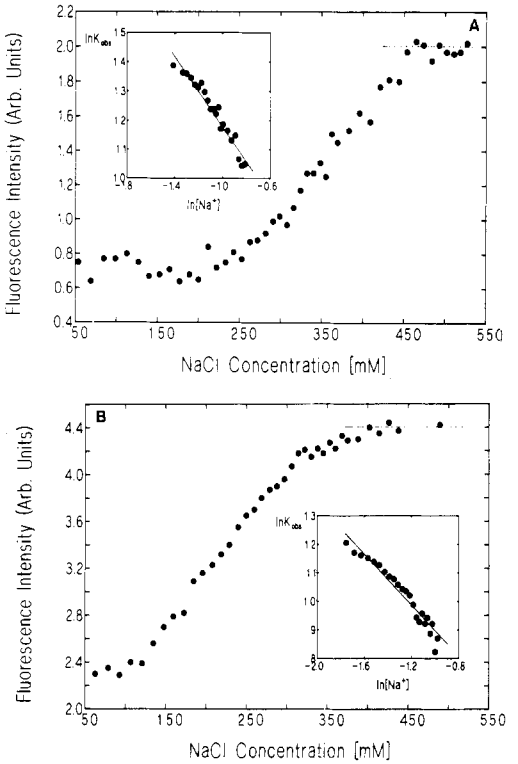

FIGURE 8: Effect of NaCl on the fluorescence intensity of TF1 complexes (λ_{exc} = 275 nm, λ_{em} = 305 nm). (A) TF1/SPO1 DNA [1.0 μM TF1 dimers, 22 μM (bp) DNA]. (B) TF1/CT DNA [1.0 μM TF1 dimers, 30 μM (bp) DNA]. The dashed lines indicate the values of i_0 that are used to calculate K_{obs}, as explained under Materials and the Methods. The inserts show log–log plots of K_{obs} and [Na^+] according to the method of Record et al. (1976).

Table III: Effects of Binding Ratio and Assumed Binding Site Density on the Calculated Number of Sodium Ions Dissociated upon Binding[a]

sample	c_{TF1}/c_{DNA} (μM dimers/μM bp)	assumed binding site density (n)	number of Na^+[b] (m'/ψ)
TF1/SPO1 DNA	1/22	4	7.9 ± 0.4[a]
		5	8.0 ± 0.4
		7	8.1 ± 0.4
	1/60	5	6.8 ± 1.0
TF1/CT DNA	1/29	4	5.1 ± 0.3
		5	5.2 ± 0.3
		7	5.2 ± 0.3
	1/60	5	4.0 ± 0.5

[a] Calculated by using $Q_{max} = 0.75$. [b] The uncertainties represent estimated standard deviations.

is stable at higher salt concentrations. The transition interval is also sharper with SPO1 (≈200 mM) than with CT DNA (≈300 mM), suggesting a more pronounced salt dependence in the former complex, which we now analyze in more detail.

The inserts in Figure 8 show plots of the data according to the method of Record et al. (1976a; deHaseth et al., 1977), where the logarithm of the observed binding constant, K_{obs} (calculated as described under Materials and Methods) is plotted against the logarithm of the Na^+ concentration. The slope obtained in such a plot is proportional to the (net) number of ions that are displaced upon associating one binding unit of protein with DNA. We find that binding of TF1 to SPO1 DNA displaces more ions than does binding to CT DNA. Given the value of $\psi = 0.88$ (Record et al., 1976a,b), one can estimate that about eight and five Na^+ are displaced in the SPO1 and CT DNA complexes, respectively. This

analysis is rather insensitive to the assumed value for the binding site density, n (Table III). Note, however, that these estimates of the number of ionic contacts are based on a simple binding model (eq 8) and therefore might only apply to the conditions of the experiments shown in Figure 8 (1 μM TF1 dimers/22–29 μM DNA bp). Experiments repeated at a lower TF1–DNA ratio (1 μM TF1 dimers/60 μM DNA bp) (Table III) yield somewhat lower values for the number of dissociated ions, although the difference between the CT and SPO1 DNA complexes is retained. The difference can be attributed to effects due to cooperativity and overlapping binding sites. A complete analysis of the effect of ionic strength on the TF1–DNA equilibrium would include the determination of all parameters in the McGhee–Von Hippel model (McGhee & Von Hippel, 1974) at different salt concentrations. Unfortunately, such an analysis is not possible because of uncertainties in the free ligand concentration due to protein aggregation, as discussed above. Still, the fact that the difference between the CT and SPO1 complexes is retained at the lower binding density indicates that this difference is not an artifact due to our simple model of the equilibrium.

Discussion

In this study we have employed several fluorescence methods to probe the local environment of Tyr94 in free TF1 and in TF1 bound to different DNAs and to study various aspects of the TF1–DNA interaction.

Properties of Free TF1. The fluorescence lifetime measurements on free TF1 show that the decay can be fitted by a single exponential, and this is consistent with a symmetrical dimer structure with two equivalent Tyr94 residues per dimer. While this is reasonable, the results of Searcy et al. (1988) on a tetrameric protein show that this is not always true. Studies using a variety of quenchers reveal that the Tyr94 residue is exposed in free TF1 (as evidenced by the acrylamide quenching constant). Tyr94 is less effectively quenched by negative ions such as I^- or citrate, and we attribute this to electrostatic effects arising from negatively charged residues in TF1 located near Tyr94. The Tyr94 fluorescence intensity and steady-state polarization and acrylamide quenching constants are concentration dependent, and from this we infer that there is intermolecular association of the TF1 dimers in a concentration range extending from 2.5 to 500 μg/mL. This intermolecular association equilibrium complicates detailed analyses of the TF1–DNA equilibrium.

Properties of TF1 Complexes with SPO1 and CT DNA. Previous studies, as well as the present work, show that the interaction of TF1 with SPO1 DNA is complex. At very low protein concentrations (ca. 0.5–5 $\times$ 10^{-9} M, at ca. 18 °C in a buffer containing 100 mM Tris-HCl, pH 8, 10 mM $MgCl_2$, 50 mM NaCl, and 8% glycerol) TF1 occupies a limited number of preferred binding sites that are relatively widely spaced along the SPO1 genome. This binding has two principal characteristics: (i) It is hmUra specific as well as sequence specific. (ii) It involves nested sets of protein–DNA complexes, i.e., occupancy of a core DNA site at the lowest TF1 concentration and lateral spreading of binding from that core to adjacent DNA as the protein concentration increases. Several, but not all, of the preferred binding sites that have been analyzed overlap SPO1 early promoters (Greene & Geiduschek, 1985a; Greene et al., 1986). This is probably the reason why TF1 blocks transcription of SPO1 DNA by bacterial RNA polymerase (Wilson & Geiduschek, 1969; Geiduschek et al., 1977). The strongest binding sites have certain common sequence features but no simple consensus. It has been suggested that the local conformation of DNA or its local deformability might be the dominant determinants of site-specific binding (Greene et al., 1986). As the protein concentration is increased, additional binding sites with weaker affinities are occupied (Greene & Geiduschek, 1985b). An analysis of the binding at higher TF1 concentrations (20 °C in 10 mM phosphate, pH 7.5, and 150 mM KCl) by short column centrifugation yielded a binding isotherm apparently saturating at approximately 1 TF1 dimer/DNA 60 bp, with half-saturation at ca. 3 $\times$ 10^{-8} M free TF1 dimer. It was established that the affinity for thymine-containing DNA, of nonidentical sequence, was approximately 15-fold weaker (Johnson & Geiduschek, 1977).

In the present experiments we find that by raising the TF1 concentration more than an order of magnitude and by lowering the electrolyte concentration to 50 mM NaCl, 10 mM Tris-HCl, and 2 mM Na_2EDTA at pH7 the amount of TF1 capable of binding to SPO1 DNA can be increased almost 10-fold, yielding complexes containing ca. 5 g of protein/g DNA (at saturation). At this binding density, binding is not selective for hmUra-containing SPO1 DNA (the affinity for CT DNA appears, in fact, to be somewhat higher than for SPO1 DNA in Figure 7A). Nevertheless, even here there are differences between the two complexes: (i) TF1 appears to make more electrostatic contacts with SPO1 DNA than with CT DNA (Figure 8). (ii) SPO1 and CT DNA binding provide different environments around Tyr94 on TF1 as judged by the different D_2O effects on Tyr94 in the two complexes. (iii) Tyr94 is considerably more susceptible to acrylamide quenching in the complex with CT DNA than it is in the SPO1 DNA complex. The following analysis provides additional information about the spatial location of Tyr94 in the various TF1–DNA complexes we have studied.

Mechanisms of Tyrosine Fluorescence Quenching and Structural Implications. Fluorescence quenching is often observed when aromatic amino acids bind to DNA (Hélène, 1971; Hélène & Dimicoli, 1972; Brun et al., 1975; Motenay-Garestier, 1975). With tyrosine, there are several possible mechanisms that might affect the fluorescence quantum yield: (i) Hydrogen bonding between the hydroxyl proton on tyrosine and acceptors on DNA (Sellini et al., 1973) can probably be ruled out as judged from the absence of broadening of the emission peak upon binding (Lakowicz, 1984). Hydrogen-bonding interactions with the DNA phosphates are also unlikely because such interactions are not expected to result in fluorescence quenching (Alev-Behmoaras et al., 1979). (ii) Stacking (intercalation) interactions with the DNA bases can also be ruled out because this type of tyrosine binding has only been observed with single-stranded polynucleotides [poly(A) or denatured DNA], where it completely quenches the fluorescence (Hélène & Dimicoli, 1972). (iii) Feitelson (1964) has proposed that electron transfer from tyrosine to nearby weak acids (such as carboxylic groups and hydroxylamines) causes quenching. Little else seems to be known about this mechanism, but the absence of weakly acidic groups on DNA at pH 7 makes its relevance less probable. (iv) Feitelson also found that the electron-transfer mechanism can be "overshadowed" by quenching through catalyzed exchange of the hydroxyl proton in the presence of weak bases. Regarding this mechanism, it is interesting to note that a D_2O effect on the quantum yield is not expected unless exchange of the tyrosine proton is base-catalyzed. This is because the exchange rate in excited-state tyrosine is on the order of 10^5 s^{-1} (Feitelson, 1964), which is slow compared to the fluorescence decay rate. The fluorescence quantum yield is therefore insensitive to deuterium effects on the uncatalyzed rate constant, as ar-

gued by Stryer (1966). The presence of a catalyst will increase the exchange rate, and a deuterium effect is likely to be observed. Our results therefore suggest the presence of catalyzed proton exchange with neighboring weak bases (maybe Glu95 or Asp96) in free TF1 and in TF1 bound to SPO1 DNA. (v) Energy transfer between tyrosine and the DNA bases is likely to contribute to the quenching. Calculations of singlet energy-transfer rates show that critical Förster distances are large enough (R_0 = 10–15 Å) in natural DNAs to cause quenching of a tyrosine residue bound in one of the DNA grooves (Montenay-Garestier, 1975). Our results, presented in Figure 6, show that energy transfer contributes significantly to the quenching of the Tyr94 fluorescence in the bound state, and this indicates that the tyrosine residue is located "in the vicinity" of the bases in the TF1–DNA complex.

In order to calculate the effective distance between the Tyr94 residue and the DNA bases from the data in Figure 6B, we need to make assumptions regarding the position of the tyrosine relative to the DNA helix axis, the orientation of tyrosine and DNA bases, transition moment directions, and the local mobility of the tyrosine in the bound state, as well as assumptions regarding the extent of quenching by mechanisms other than energy transfer. If we assume that a single DNA base pair acts as an isolated chromophore (acceptor) and that energy transfer is the dominant quenching process, then we estimate the effective distance between the center of this base pair and the Tyr94 residue is about 10–11 Å for the various DNAs we studied. (In these calculations we use an orientation factor $\kappa^2 = {}^2/_3$, a refractive index n = 1.35, and a quantum yield of TF1 fluorescence ϕ_f = 0.07.) If we take into account contributions of neighboring base pairs as acceptors, then the effective distance will increase. A calculation of the effective distance from an array of acceptors is complicated, but the effect of neighboring base pairs is expected to converge rapidly, because the energy-transfer rate varies inversely with the sixth power of the distance. (Note that inclusion of the effect of neighboring base pairs diminishes the errors that might be introduced by assuming $\kappa^2 = {}^2/_3$.) If we assume that other mechanisms cause a ≈40% reduction in fluorescence quantum yield upon binding, as evidenced in Figure 6B, then the critical distance, R_0, is reduced with a factor of $(0.60)^{1/6} = 0.92$, but the fraction of quenching due to energy transfer is also reduced. For SPO1 DNA these effects cancel, so that the calculated effective distance is still ≈11 Å for the case with a single base pair acting as energy acceptor. Alternatively, a calculation of the effective Förster distance using eq 5 (in which the effect of other mechanisms is included) and all data points in Figure 6B also yields a distance of ≈11 Å. These arguments place a lower limit of 10–11 Å for the distance between the Tyr94 residue and the closest DNA base pair. On the other hand, it would be difficult to account for these results if the distance were greater than 13–14 Å. We therefore conclude that excitation energy transfer contributes significantly to the quenching of Tyr94 fluorescence in the TF1–DNA complexes and that the approximate magnitude of the effect places this residue within 10–14 Å of the DNA helix axis. If there were direct contact between Tyr94 and the DNA bases in any of the complexes, complete quenching of the Tyr94 fluorescence would have been expected. We therefore also conclude that direct interaction of Tyr94 and DNA bases is not playing an essential role in the nonspecific recognition of SPO1 DNA, at high binding densities.

We do find evidence for differences between the TF1 complexes with SPO1 and CT DNA, although the average distance between Tyr94 and the DNA bases appears to be approximately the same in the two complexes. More ionic contacts contribute to TF1 binding to SPO1 DNA than to CT DNA, and Tyr94 is more protected from solvent exposure in the TF1-SPO1 DNA complex. These effects might therefore be due to other factors, such as differences in protein–protein interactions in the bound state. It seems likely that the observed differences are caused by the presence of the "extra" hydroxymethyl group in the major groove of SPO1 DNA. The hmUra could either affect the fluorescence properties of Tyr94 "directly" if the tail binds in the DNA major groove or "indirectly" by favoring an orientation of TF1 on DNA that results in an altered TF1 conformation or in specific interactions between the tails of neighboring protein molecules. The first of these alternatives seems less likely if the Tyr94 is indeed located 10–14 Å from the helix axis, unless the tail binds to the DNA with the Tyr94 facing out towards the solvent. The second alternative (protein–protein interactions) is supported by the observations that the Tyr94 is less exposed to the solvent and the fluorescence is quenched at high concentrations of free protein where TF1 seems to aggregate. In this case additional quenching and differences in the effect of D_2O on CT and SPO1 DNA complexes could arise from proton or electron transfer in a tail–tail complex.

Two additional and independent lines of evidence about TF1–DNA interactions are worth noting in this context: (i) Recent footprinting experiments with wild-type TF1 and a mutant lacking the nine C-terminal amino acids have shown that this tail is essential for site-specific TF1 binding (Sayre & Geiduschek, 1988). (ii) Model-building studies (using molecular graphics) show that the tails of the TF1 dimer can be placed in close proximity (10–14 Å) to the DNA when the arms bind the DNA (V. Hsu, unpublished results). The model-building studies also indicate that the tails of two TF1 dimers bound next to each other are likely to interact. The present studies, taken together with footprinting experiments and model-building studies, are therefore consistent with a TF1–DNA complex where the tail is located in close proximity with the DNA (but the Tyr94 residue is not in direct contact with the DNA bases) and where the interactions of the tail, maybe with neighboring proteins, are important to the structure and function of the complex and the local environment of the Tyr94 residue.

Registry No. Poly(dAdU), 34607-75-5; poly(dAI^5dU), 59164-41-9; poly(dIdC), 34639-43-5; poly(dIBr^5dC), 51853-68-0; L-tyrosine, 60-18-4; deuterium, 7782-39-0.

References

Alev-Behmoaras, T., Toulme, J. J., & Hélène, C. (1979) *Photochem. Photobiol. 30*, 533–539.

Brun, F., Toulme, J. J., & Hélène, C. (1975) *Biochemistry 14*, 558–563.

Buckley, K. (1985) Ph.D. Thesis, University of California, San Diego.

Bujalowski, W., & Lohman, T. M. (1987) *Biochemistry 26*, 3099–3106.

Bulsink, H., Harmsen, B. J. M., & Hilbers, C. W. (1985) *J. Biomol. Struct. Dyn. 3*, 227–247.

Cantor, C. R., & Schimmel, P. R. (1980) in *Biophysical Chemistry*, Part III, Freeman, San Francisco.

Cazenave, C., Tolume, J. J., & Hélène, C. (1984) *EMBO J. 2*, 2247–2251.

Chen, R. F. (1967) *Anal. Lett. 1*, 35–42.

deHaseth, P. L., Lohman, T. M., & Record, M. T. (1977) *Biochemistry 16*, 4783–4790.

de Jong, E. A. M., Harmsen, B. J. M., Konings, R. N. H., & Hilbers, C. W. (1987) *Biochemistry 26*, 2039–2046.
Dijk, J., White, S. W., Wilson, K. S., & Appelt, K. (1983) *J. Biol. Chem. 258*, 4003–4006.
Eftink, M. R., & Ghiron, C. A. (1976) *Biochemistry 15*, 672–680.
Feitelson, J. (1964) *J. Phys. Chem. 68*, 391–397.
Förster (1948) *Ann. Phys. 2*, 55–79.
Geiduschek, E. P., Armelin, M. C. S., Petrusek, R., Beard, C., Duffy, J. J., & Johnson, G. G. (1977) *J. Mol. Biol. 118*, 825–842.
Greene, J. R., & Geiduschek, E. P. (1985a) *EMBO J. 4*, 1345–1349.
Greene, J. R., & Geiduschek, E. P. (1985b) in *Sequence Specificity in Transcription and Translation* (Gold, L., & Calendar, R., Eds.) pp 255–269, Liss, New York.
Greene, J. R., Brennan, S. M., Andres, D. J., Thompson, C. C., Richards, S. H., Heinrikson, R. L., & Geiduschek, E. P. (1984) *Proc. Natl. Acad. Sci. U.S.A. 81*, 7031–7035.
Greene, J. R., Morrissey, L. M., Foster, L. M., & Geiduschek, E. P. (1986) *J. Biol. Chem. 261*, 12820–12827.
Greene, J. R., Appelt, K., & Geiduschek, P. E. (1987) in *DNA: Protein Interactions and Gene Regulation* (Thompson, E. B., & Papaconstantinov, J., Eds.), The University of Texas, Austin.
Hélène, C. (1971) *Nature (London) 234*, 120–121.
Hélène, C., & Dimicoli, J. L. (1972) *FEBS Lett. 26*, 6–10.
Johnson, G. G., & Geiduschek, E. P. (1972) *J. Biol. Chem. 242*, 3571–3578.
Johnson, G. G., & Geiduschek, E. P. (1974) *Methods Enzymol. 29E*, 204–215.
Johnson, G. G., & Geiduschek, E. P. (1977) *Biochemistry 16*, 1473–1485.
Khrapunov, S. N., Sivolob, A. V., & Kucherenko, N. E. (1984) *Int. J. Biol. Macromol. 6*, 199–202.
Kowalczykowski, S. C., Lonberg, N., Newport, J. N., & von Hippel, P. H. (1981) *J. Mol. Biol. 145*, 75–104.
Lakowicz, J. R. (1984) in *Principles of Fluorescence Spectroscopy*, Plenum, New York.
Lakowicz, J. R., Laczko, G., & Gryczynski, I. (1987) *Biochemistry 26*, 88–90.
Laws, W. R., Ross, J. B. A., Wyssbrod, H. R., Beechem, J. M., Brand, L., & Sutherland, J. C. (1986) *Biochemistry 25*, 599–607.
Lawson, R. C., & York, S. S. (1987) *Biochemistry 26*, 4867–4875.
Libertini, L. J., & Small, E. W. (1985) *Biophys. J. 47*, 765–772.
McGhee, J. D., & Von Hippel, P. H. (1974) *J. Mol. Biol. 86*, 469–489.
Miller, J. H. (1972) in *Experiments in Molecular Genetics*, Appendix I, Cold Spring Harbor Laboratory, Cold Spring Harbor, NY.
Montenay-Garestier, T. (1975) *Photochem. Photobiol. 22*, 3–6.
O'Connor, D. V., & Phillips, D. (1984) in *Time-correlated Single Photon Counting*, pp 180–189, Academic, Orlando, FL.
Press, W. H., Flannery, B. P., Teukolsky, S. A., & Vetterling, W. T. (1986) in *Numerical Recipes*, Chapter 14, Cambridge University, Cambridge, England.
Record, M. T., Lohman, T. M., & de Haseth, P. (1976a) *J. Mol. Biol. 107*, 145–158.
Record, M. T., Woodbury, C. P., & Lohman, T. M. (1976b) *Biopolymers 15*, 893–915.
Sayre, M. H., & Geiduschek, E. P. (1988) *J. Virol.* (in press).
Searcy, D. G., Montenay-Garestier, T., Laston, D. J., & Hélène, C. (1988) *Biochim. Biophys. Acta 953*, 321–333.
Sellini, H., Maunzot, J. C., Dimicol, J. L., & Hélène, C. (1973) *FEBS Lett. 30*, 219–224.
Skibsted, L. H., Hancock, M. P., Magde, D., & Sexton, D. A. (1987) *Inorg. Chem. 26*, 1708–1712.
Stryer, L. (1966) *J. Am. Chem. Soc. 88*, 5708–5712.
Tanaka, I., Appelt, K., Dijk, J., White, S. W., & Wilson, K. S. (1984) *Nature (London) 310*, 376–381.
Wahl, P. (1979) *Biophys. Chem. 10*, 91–104.
Wilson, D. L., & Geiduschek, E. P. (1969) *Proc. Natl. Acad. Sci. U.S.A. 62*, 514–520.